

either tip diameter or electrode resistance be minimized. Figure 2 shows for our electrodes that, when either tip diameter or electrode resistance has been reduced to a given low value, further decreases can be obtained only at the expense of a very marked and undesirable increase in the other variable.

Ogden (7) finds his beveled electrodes to be more fragile than un-beveled controls when tested in monkey retinas; his beveled electrodes likewise break more readily than controls when cleaned by sonication, as revealed by a reduction of the electrode resistance after breaking. By contrast, we have found no sign of special fragility of the beveled tip, many retinal penetrations being possible in the snapping turtle with no decrease in the penetrating ability of the electrode. Also, during sonication our beveled electrodes proved no more fragile than control electrodes of similar tip size, when electrical resistance was used to match tip size and detect tip breakage. These results suggest that the tip becomes fragile during slow grinding, probably because much flexing weakens the glass. The avoidance of such fragility seems a major advantage of our rapid grinding method.

In the first trial of our beveled electrodes in a snapping turtle eyecup preparation, approaching from the vitreous humor by a Kopf stepping microdrive, we made a single retinal penetration with each of three electrodes with resistances ranging from 80 to 100 megohms (about 0.1 to 0.2 μm in tip diameter). During each electrode track we obtained intracellular recordings in sequence from a ganglion cell, then from either one or two horizontal cells of the inner nuclear layer, and finally from a photoreceptor. At the end of the third electrode track the photoreceptor recorded from was a cone, as determined by its very small receptive field, its spectral response curve, and the time course of its response to light. In this cell both the resting membrane potential and the light response were entirely stable for 4½ hours. By comparison with conventional electrodes of considerably higher resistance in the same preparation, this consistency of cell penetration and the stability of the intracellular cone response represent dramatic improvements. We infer that the greater response stability results from the beveled electrode cutting a precise aperture through the membrane that is then sealed by the electrode tip.

These advantages of beveled electrodes have been fully confirmed in other experiments.

In many small cells of great interest, intracellular recording by conventional electrodes has remained a somewhat marginal technique. The inner segments of snapping turtle photoreceptors, for example, are about 8 to 12 μm in diameter. In these cells intracellular recording, as applied to photoreceptors to date, is now so reliable that we have even used the technique successfully for a live teaching demonstration. We thus anticipate that for such cells beveled electrodes will bring within technical reach a variety of crucial experiments that have not been possible with conventional electrodes.

At one extreme beveling may be used to increase the diameter of an electrode tip as much as possible while still penetrating a given cell without significant damage. By thus reducing the electrode's electrical resistance, the signal-to-noise ratio is improved for recording small signals. The injection of marker dyes, such as Procion yellow, is also facilitated. Conventional electrodes must have a minimum resistance of about 200 megohms to penetrate well in snapping turtle photoreceptors, but we have already obtained good results from beveled electrodes with resistances as low as 50 megohms. This suggests that beveled double-barreled electrodes for voltage clamping studies should also penetrate readily in this penetration, providing that the beveling axis is appropriately controlled. Relatively large beveled electrodes are also promising for cells covered by connective tissue, since the stiffer but very sharp tip should assist penetration to the cell of interest.

At the other extreme, beveling may be applied to the smallest electrode tips

possible to maximize the ease and subtlety of cell penetration. Our experience suggests that this approach would make intracellular recording possible for smaller cells, or smaller parts of cells, than hitherto possible. The range of potential applications in this class is especially great. In retinal work the selection of species is ideally made by criteria other than cell size, partly because the details of retinal circuitry vary greatly between species. The mammalian retina is of special interest, as is the entire mammalian central nervous system, but most cells of these tissues have been too small for intracellular recording by conventional electrodes. Beveling now offers a promising approach to this problem.

KENNETH T. BROWN

DALE G. FLAMING

Department of Physiology,
University of California,
San Francisco 94143

References and Notes

1. J. N. Barrett and K. Graubard, *Brain Res.* **18**, 565 (1970); J. Barrett and D. G. Whitlock, in *Intracellular Staining in Neurobiology*, S. B. Kater and C. Nicholson, Eds. (Springer-Verlag, New York, 1973), p. 297; D. Van Essen and J. Kelly, in *ibid.*, p. 189; M. L. Shaw and D. R. Lee, *J. Appl. Physiol.* **34**, 523 (1973).
2. B. R. Kripke and T. E. Ogden, *Electroencephalogr. Clin. Neurophysiol.* **36**, 323 (1974).
3. Both products are made by the Flecto Company, Inc., Oakland, Calif. 94608.
4. K. T. Brown and D. G. Flaming, in preparation.
5. Our two-stage puller is made by Industrial Science Associates, Inc., Ridgewood, N.Y. 11227. It has been modified to provide a 25-second delay between the time when the heating coil is turned on and the onset of the slow pull. The Livingstone puller is made by Otto K. Hebel, Scientific Instruments, Rutledge, Pa. 19071.
6. K. Tasaki, Y. Tsukahara, S. Ito, M. J. Wayner, W. Y. Yu, *Physiol. Behav.* **3**, 1009 (1968).
7. T. E. Ogden, personal communication.
8. This work was supported by grant No. EY-00468 from the National Eye Institute. We thank J. R. Wall and S. Winston for constructing the grinding equipment and M. T. Maglio for assistance with the scanning electron microscopy.

11 April 1974; revised 24 May 1974

Eolian Biogenic Detritus in Deep Sea Sediments: A Possible Index of Equatorial Ice Age Aridity

Abstract. Opal phytoliths and freshwater diatoms, transported mainly in dust to the equatorial Atlantic, are common in sediments deposited when ocean waters were cool, and sparse in those deposited when waters were warm, during the last 1.8 million years. Climate in source areas of the southern Sahara apparently was more arid during glacial and more humid during interglacials.

Dust transported from Africa by the trade winds to the equatorial Atlantic has been studied for more than 100 years (1-3). However, until recently (4, 5) little work has focused on the abundance of biogenous and terrigenous

components of the dust in equatorial deep sea cores, where variations document changes with time in source areas that can be compared with oceanic temperature fluctuations. To investigate the potential of such comparisons we

measured concentrations of opal phytoliths (6) and freshwater diatoms in three cores that have well-studied oceanic faunal records (7, 8). These land-derived components are mainly transported by wind (3), are relatively easy to identify, seem to be resistant to solution, and are sensitive indicators of continental climate. The cores sampled were collected in 1968 from the U.S.N.S. *Kane* near the Cape Verde Islands and include: K9-57 (8°38'N;

22°02'W), K9-30 (19°40.9'N; 24°-35.9'W), and K9-34 (21°03.5'N; 28°-02.1'W) (Fig. 1). Because the study was conducted at a reconnaissance level, most samples were collected at fairly wide intervals; more detail is now being acquired. Core K9-57 lies near the axis of present high winter dust transport from North Africa, whereas K9-30 and K9-34 lie in the area of high summer dust transport (1, 3). Ruddiman (7, 8) established the

faunal boundary zones of all three cores and the magnetic stratigraphy of K9-57.

We removed carbonate from each sample (1 to 6 g) and passed the weighed residue through a Buckbee-Mears Micromesh 10- μ m sieve (nominal 8 to 12 μ m) during sonication. (Most phytoliths and diatoms have intermediate diameters that exceed 10 μ m.) A portion of the material in the size range greater than 10 μ m was placed on a clean glass slide, dried, and mounted in Caedex (synthetic Canada balsam; index of refraction $n_d^{20^\circ C} = 1.56$). The slide was scanned under a polarizing microscope ($\times 250$ to $\times 500$) for Festucoid, Chloridoid, Panicoid, and Elongate phytoliths (9), for the freshwater diatoms *Melosira* and *Stephanodiscus astrea*, and, in five samples, for anisotropic mineral grains. The concentrations of the components are given as the number in the size range greater than 10 μ m per gram of total $CaCO_3$ -free sediment.

The 23.5 m of sediment in K9-57 spans the Pleistocene and Holocene epochs. The core is well located for evaluating variations with time of the detritus transported by wind from Africa; it apparently contains no turbidites (7) despite its position along the flank of a fracture zone (10). The concentration of wind-transported biogenic components (phytoliths plus diatoms) is consistently low ($< 8 \times 10^4 g^{-1}$) before 1.1 million years ago, but thereafter ranges widely in about eight cycles from as few as $0.1 \times 10^4 g^{-1}$ to as many as $59 \times 10^4 g^{-1}$ with a mean of $12.2 \times 10^4 g^{-1}$ (Fig. 2). Phytolith specimens in the Elongate and Panicoid classes are abundant, whereas those in the Chloridoid and Festucoid classes are comparatively rare. The freshwater diatom *Melosira* is the most common component; *Stephanodiscus* is the least common. The shape of the curve generated by each component is generally similar to the total component curve. Concentrations of mineral grains $> 10 \mu$ m (mostly quartz) increase and decrease with those of the biogenic components in the five samples evaluated; the values range from 1.9×10^6 to $5.4 \times 10^6 g^{-1}$. Median diameters are close to 18 μ m for the intermediate axes and close to 21 μ m for the long axes.

We examined only 6 samples from K9-30 and 12 samples from K9-34 (Fig. 1). In K9-30, the total concentrations of phytoliths plus diatoms range from 0.3×10^4 to $3.8 \times 10^4 g^{-1}$ with a

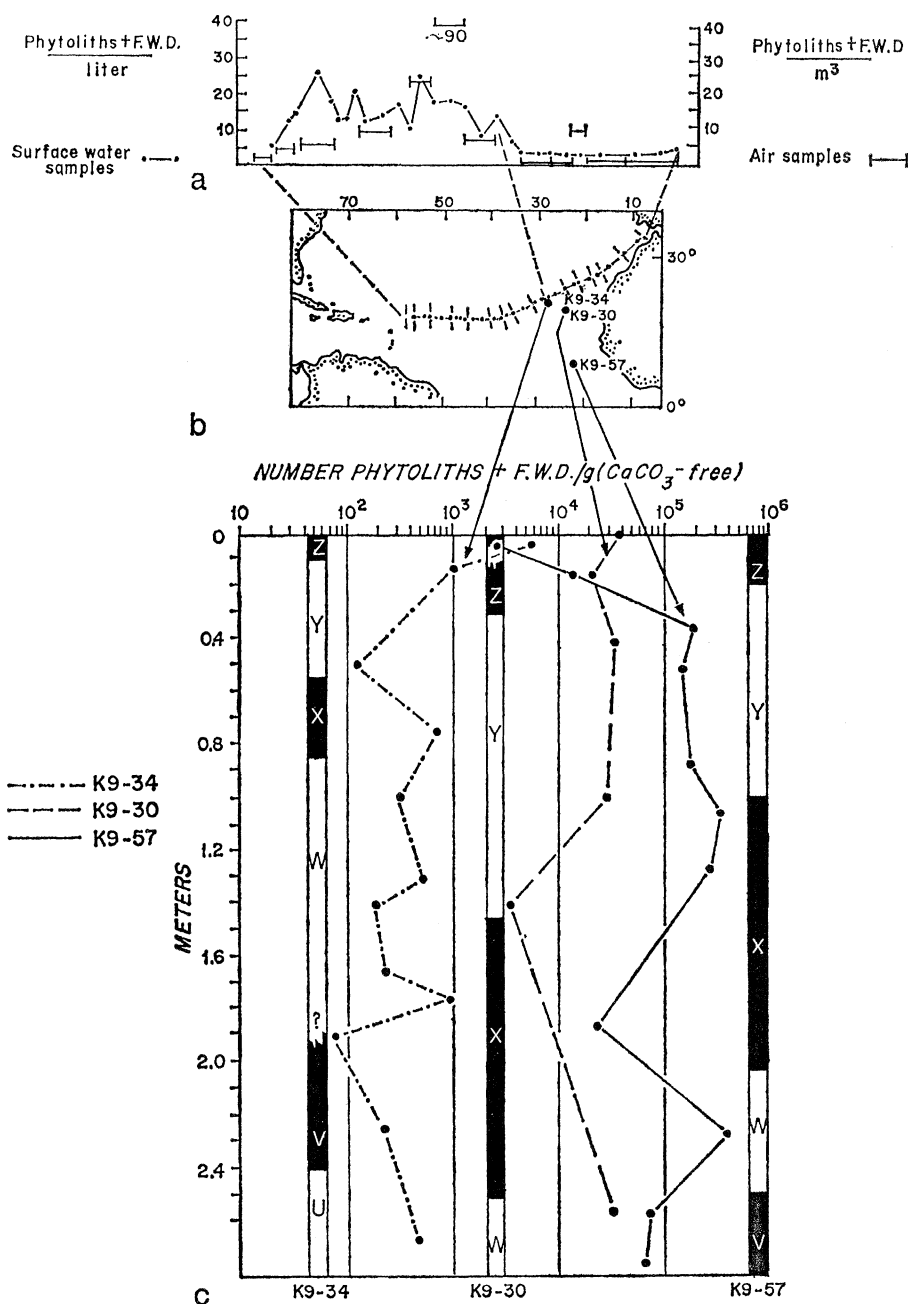


Fig. 1. (a and b) The abundance of eolian land-derived components, opal phytoliths and freshwater diatoms (F.W.D.), decreased to the north in air samples (bars) and surface water samples (small black dots) collected in 1965 along the track of the H.M.S. *Vidal* (3). (c) We have observed a similar decrease in the concentrations (large black dots) of grass phytoliths and freshwater diatoms in the size range greater than 10 μ m in deep sea sediment; these components are highest in core K9-57 and lowest in core K9-34 [see (b)]. The climatic zones X, Y, and Z were determined by Ruddiman (7, 8) after Ericson and Wollin (13).

mean of $2.8 \times 10^4 \text{ g}^{-1}$. Among the phytoliths, those in the Elongate and Festucoid classes are most common. *Melosira* is present in all but one sample, but *Stephanodiscus* is absent in all but one sample. *Melosira*, Elongate, and Festucoid components display similar concentration trends. In K9-34, phytoliths and diatoms are rare and range from 0.01×10^4 to $0.5 \times 10^4 \text{ g}^{-1}$ with a mean of $0.09 \times 10^4 \text{ g}^{-1}$. Only one sample, at 5 cm, contains representatives of as many as three groups (Chloridoid, Panicoid, and *Melosira*). The few Elongate and Festucoid phytoliths observed in the remaining 11 samples are poorly preserved and difficult to identify.

During the last 200,000 to 300,000 years, fewer land-derived biogenic materials have reached the area of K9-34 and K9-30 than have reached that of K9-57. Two factors probably account for this distribution: (i) K9-30 and K9-34 lie near the northern limit of present dust transport from Africa (1-3), and (ii) less biogenic detritus has probably been available from the more arid northern Sahara than from the semiarid southern Sahara (see Fig. 1). A dust fall, for example, that occurred between the Cape Verde and Canary Islands ($26^\circ 50' \text{N}$; $21^\circ 04' \text{W}$) contained significantly fewer phytoliths and diatoms relative to quartz (11) than a fall that occurred south of the Cape Verde Islands (12).

The concentrations of phytoliths and diatoms have been plotted with Ruddiman's (7) "total fauna climatic curve" for K9-57 (Fig. 2). The low values before about 1.1 million years ago correlate well with a period of relative warmth and apparent oceanic temperature stability. Afterwards, concentrations range widely, with maxima coincident with or slightly preceding high percentages of excess cool species and minima coincident with or slightly preceding high percentages of excess warm species. Variations in the upper 5 m (about 300,000 years ago), where we have the most data, correlate best with Ruddiman's curve. The changes with time of concentrations in K9-57 and K9-30 are broadly similar, high values occurring in the Y and W climatic zones (13) and low values in the X and Z zones, except for samples near boundaries and, of particular note, the most recent sample in K9-30; counts from K9-34 are low and vary erratically (Fig. 1).

The mineral grain content in the five samples from K9-57 is about twice

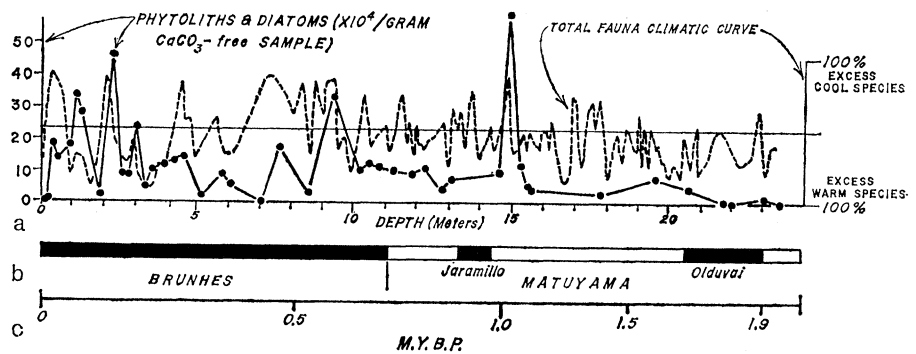


Fig. 2. (a) High concentrations of land-derived eolian components in the size range greater than $10 \mu\text{m}$ (black dots) most often coincide with high percentages of cooler-water fauna (dashes) (7) in deep sea core K9-57. Dust transport increased at the onset of and during glacials. (b) Magnetic reversals were determined by Ruddiman (7). (c) The time scale is Opdyke's (18); M.Y.B.P., million years before present.

as high during cold periods as during warm periods. If these counts are representative of other variations in the core, as Bowles's (4) data suggest, then windblown terrigenous material increased with, but not as much as, windblown biogenic material during cold periods. Soil apparently was more available for deflation during glacials than during interglacials.

Variations in wind velocity (4), wind direction (14), and aridity (see below) all may account in part for the differences observed. However, mineral grain concentrations ($> 10 \mu\text{m}$) decreased by only a factor of about 2 from cold to warm periods, whereas phytolith and diatom concentrations decreased by as much as a factor of 50 in the same five samples. Fluctuations of available moisture in the source area appear to be essential to account for the greater variability of the biogenic constituent concentrations.

Data derived from a variety of continental and a few oceanic observations support the concept of more widespread aridity rather than humidity in the equatorial region during much of the last glacial [see (14-16) and references therein]. The following interpretation of our data supports this hypothesis: At the onset of an interglacial (or warm period), moisture became more available, grass cover increased, and lakes, such as Chad, enlarged (15, 17). Thus, freshwater diatoms in lake sediments were more often covered by water, phytoliths were more often bound up in a vegetal mat, and, because less soil was exposed to wind erosion, the total dust load declined. With the subsequent onset of a glacial (or cool period), moisture decreased, vegetation was reduced,

lakes contracted, and soil with abundant phytoliths and diatoms, accumulated mainly during the previous interglacial, was exposed and deflated. In this model, more biogenic detritus should be present in dust transported at the onset of glaciation. This is perhaps illustrated by a number of samples from K9-57 in cycles where phytoliths and diatoms appear to reach their highest concentrations slightly before oceanic temperatures reach their lowest values.

In summary, we attribute higher concentrations of dust in equatorial sediments during cool periods or transitions to them at least in part to increased desiccation of the Saharan region. Thus, the recent disastrous drought that has spread throughout equatorial Africa may be a limited example of more extensive aridity that will characterize the area during much of the next high-latitude glacial advance.

CAROL PARMENTER
D. W. FOLGER

Department of Geology,
Middlebury College,
Middlebury, Vermont 05753

References and Notes

1. C. G. Ehrenberg, *Abh. Preuss. Akad. Wiss.* (1847), p. 269; G. Hellmann, *Mber. K. Preuss. Akad. Wiss. Berlin* (1878), p. 364; O. Pratje, *Zentralbl. Mineral. Geol. Palaeontol. Abt. B* 4, 177 (1934); J. M. Prospero and T. J. Carlson, *J. Geophys. Res.* 77, 5255 (1972).
2. A. C. Delany, A. C. Delany, D. W. Parkin, J. J. Griffin, E. D. Goldberg, B. E. F. Reimann, *Geochim. Cosmochim. Acta* 31, 885 (1967).
3. D. W. Folger, *Deep-Sea Res.* 17, 337 (1970).
4. F. A. Bowles, *Trans. Am. Geophys. Union* 54, 328 (1973).
5. E. Bonatti, *ibid.*, 327; C. Parmenter and D. W. Folger, *ibid.*, p. 327.
6. Opal phytoliths are minute silica bodies precipitated in the epidermal cells of many land plants, especially, in this case, prairie grasses (9).
7. W. F. Ruddiman, *Bull. Geol. Soc. Am.* 82, 283 (1971).
8. ———, personal communication. Faunal data for K9-30 and K9-34 have not yet been pub-

- lished. Neither core was aligned when extruded; hence, no magnetic stratigraphy is available.
9. P. C. Twiss, E. Suess, R. M. Smith, *Soil. Sci. Soc. Am. Proc.* **33**, 109 (1969).
 10. J. Egluff, *Am. Assoc. Petrol. Geol. Bull.* **56**, 694 (1972).
 11. The dust fall sample was provided by J. H. Kravitz of the U.S. Naval Oceanographic Office and collected by T. Drobog of the S.S. *Rio San Juan*.
 12. D. W. Folger, L. H. Burckle, B. C. Heezen, *Science* **155**, 1243 (1967).
 13. D. B. Ericson and G. Wollin, *ibid.* **162**, 1227 (1968).
 14. R. W. Fairbridge, in *Problems in Paleoclimatology*, A. E. M. Nairn, Ed. (Interscience, New York, 1964), p. 356; *Quat. Res.* **2**, 283 (1972).
 15. K. W. Butzer, G. L. Isaac, J. L. Richardsen, D. Washbaum-Kamau, *Science* **175**, 1069 (1972).
 16. R. F. Flint, *Glacial and Quaternary Geology* (Wiley, New York, 1971), p. 892; J. E. Dammuth and R. W. Fairbridge, *Bull. Geol. Soc. Am.* **81**, 189 (1970); E. M. Van Zinderen Bakker, *Paleobotanist* **15**, 128 (1966); in *Background to Evolution in Africa*, W. W. Bishop and J. D. Clarke, Eds. (Univ. of Chicago Press, Chicago, 1967), p. 125.
 17. H. Franz, in *Background to Evolution in Africa*, W. W. Bishop and J. D. Clarke, Eds. (Univ. of Chicago Press, Chicago, 1967), p. 273.
 18. N. D. Opdyke, *Rev. Geophys. Space Phys.* **10**, 213 (1972).
 19. We thank W. F. Ruddiman, E. D. Schneider, P. R. Vogt, and F. A. Bowles of the Naval Oceanographic Office for allowing and helping us to sample the cores collected from the U.S.N.S. *Kane*, J. B. Folger for translations, and E. W. Coneybear for drafting assistance. The U.S. Geological Survey supported part of the manuscript preparation. Drs. Ruddiman and Burckle kindly reviewed the manuscript and provided useful suggestions.

23 October 1973; revised 4 January 1974 ■

Glacial Migrations of Plants: Island Biogeographical Evidence

Abstract. *Analyses of the floras of the high north Andean habitat islands (paramos) and the Galápagos Islands show that plant species diversity conforms to the MacArthur and Wilson model of island biogeography but that immigration occurred primarily during glacial periods. Modern plant species diversity is more significantly correlated with area and distance measures of the glacial forms of the islands than with similar measures of the present-day islands.*

According to the MacArthur and Wilson (1) theory of island biogeography (2), the number of species on an oceanic island, or on a continental habitat island (1-3), is primarily correlated to, and a function of, the area of that island and its distance from a source of propagules. This relation holds only when enough time has elapsed to allow an approach toward an equilibrium state, or a balance be-

tween constant rates of immigration and extinction (1, 2). Assuming that there is such an equilibrium, a function of S (species number), unique for each set of islands and taxonomic group, can be derived with the area of the islands and their distances from source areas as the principal independent variables. Stepwise multiple regression has been the most common method employed for determining this function

Table 1. Results of multiple regression analyses. All analyses were made with BMD-02R, UCLA biomedical computer programs. The islands are shown in Figs. 1 and 2; S is the number of species. In parts (a) and (b) the abbreviations are as follows: A , planar area of island; DL , distance to nearest paramo with area ≥ 200 km²; ELE , elevation from tree line to highest peak of mountain massif; DS , distance to nearest paramo to the south; AVD , average distance to nearest two paramos; DE , distance to Ecuador. In parts (c) and (d) the abbreviations are: A , area of island; ELE , elevation of island; DNI , distance to nearest island; DSC , distance to Santa Cruz; $AADJ$, area of adjacent island; $DISA$, distance to Isabela.

Dependent variable	Independent variables in order entered into equation	R^2
(a) Modern paramo habitat islands		
S (linear)	A^{**} , DL , ELE , DS , DE , AVD	.6584
Log S (log-log)	Log A^{**} , log DL , log ELE , log AVD , log DE	.7111
S (semilog)	Log A^{**} , log DS , log AVD , log DL , log DE , log ELE	.7337
(b) Glacial paramo habitat islands		
S (semilog)	Log A^* , log ELE , log DL	.7169
Log S (log-log)	Log ELE^* , log DL , log A	.8410
S (linear)	A^{**} , ELE^* , DL	.9565
(c) Modern Galápagos Islands (16)		
S (semilog)	Log A^{**} , log DSC^* , log $AADJ$, log $DISA$; log DNI , log ELE	.7748
S (linear)	ELE^{**} , $AADJ^{**}$, DSC , $DISA$, A , DNI	.8101
Log S (log-log)	Log A^{**} , log ELE^{**} , log DNI , log DSC , log $AADJ$.8127
(d) Glacial Galápagos Islands		
S (linear)	A^* , DSC^* , DNI , ELE , $DISA$.6085
Log S (log-log)	Log A^{**} , log DSC , log ELE , log DNI^* , log $DISA$.8969
S (semilog)	Log A^{**} , log DSC^{**} , log DNI , log ELE^{**} , log $DISA^*$.9287

* Variables with a partial regression coefficient significant at $P = .05$. ** Variables with a partial regression coefficient significant at $P = .01$.

(3-7). In interpreting the results of such a regression analysis, it is important not only to obtain a high coefficient of correlation (R^2), but also to ascertain the contributions made to the equation by both area and distance measures.

Failures in previous studies to find significant correlations between area, distance, and species diversity have been ascribed to low vagility of the organisms, essentially nonconstant rates of immigration (bursts of colonization), or insufficient time for extinction to have produced an equilibrium with the modern area of an island or its present immigration rate (3, 5, 8, 9). Studies in which historical changes have been hypothesized as causal factors have involved either continental areas drastically affected by glacial phenomena (8) or islands connected directly to a mainland by glacial land bridges (9). Until now, there has been no positive evidence for the role of paleoecological events in the determination of modern species diversity in island situations where the islands were less severely altered or have not been connected to a continent since at least early Tertiary times.

This report provides evidence that in at least two situations, the continental paramo habitat islands and the oceanic Galápagos Islands, plant colonization has occurred through dynamic dispersal over unfavorable areas, but modern species diversity reflects an approach toward equilibrium achieved during glacial times. Stepwise multiple regression analyses made with the modern island parameters have shown that these parameters account for a large amount of the variation in species numbers of birds in both areas (3, 6). It was likely, therefore, that plant species diversity was also related to island area and distance measures. The point under investigation here is whether angiosperms, a less dynamic group of organisms than birds, show similar patterns of diversity or whether the modern flora shows stronger correlations with former island conditions.

In the first study, 151 plant species of the Colombian and Venezuelan paramos (Fig. 1), a large subsample of the total flora, were used in a stepwise multiple regression analysis with the variables listed in Table 1a (5). A former study of the avifauna (3) had shown that more than 95 percent of the current variation in species numbers from paramo to paramo could be accounted for by using these modern